IJNRD.ORG ISSN : 2456-4184
INTERNATIONAL JOURNAL OF NOVEL RESEARCH AND DEVELOPMENT (IJNRD) | IJNRD.ORG
An International Open Access, Peer-reviewed, Refereed Journal

ENHANCED EV CHARGING USING AN OPTIMIZED SEPIC-ZETA CONVERTER WITH WILD HORSE ALGORITHM

[1]Ananthapalli D V V Vamsi, [2]Chandramalla.Pavan Kumar, [3]Behara Radha Krishna, [4]Dr. Ch. Leela Kumari

[1]UG Student, [2] UG Student, [3] UG Student, [4] Assistant Professor
[1,2,3,4] Department of Electrical and Electronics Engineering,
[1,2,3,4] Godavari Institute of Engineering and Technology (Autonomous), Rajahmundry, A.P., India.

Abstract: As the electric vehicle (EV) market grows, performance and reliability are becoming essential. Existing charging infrastructures often struggle with speed, energy efficiency, and performance, presenting challenges for both users and manufacturers. This paper introduces an advanced EV charging solution using a coupled inductor SEPIC-Zeta converter optimized by the Wild Horse Algorithm for enhanced proportional-integral (PI) control. This innovative system integrates a photovoltaic (PV) source with a bidirectional DC-DC converter, improving charging efficiency. The SEPIC-Zeta converter design improves energy conversion and voltage regulation, overcoming the limitations of traditional converters. Pulse-width modulation (PWM) signals maintain stable charging conditions by dynamically adjusting output voltage. The Wild Horse Algorithm optimizes PI controller parameters, improving transient response and system robustness against variations in input voltage and load. A three-phase voltage source inverter (VSI), coupled with an LC filter, ensures clean energy delivery to the grid. Through advanced control techniques and converter design, the system enhances energy management at EV charging stations and supports sustainable transportation. This paper is implemented using MATLAB Simulation 2021a.

Index Terms **– Electric Vehicle (EV) Charging; Wild Horse Algorithm; Renewable energy stability; Bidirectional DC-DC Converter**

I. INTRODUCTION

The transition to more efficient transportation can be significantly enhanced by integrating renewable energy sources into electric vehicles (EVs) [1]. Compared to hybrid cars, EVs are more eco-friendly and play a crucial role in reducing greenhouse gas emissions and combating climate change [2-4]. However, with the rapid increase in EV adoption, new challenges have emerged, particularly around charging infrastructure [5,6]. The need for fast and reliable charging stations is growing, but the integration of ultra-fast chargers depends heavily on the energy supply. Challenges such as power surges, outages, and overloads require effective solutions [7]. One promising solution is the development of a robust, adaptable charging system that utilizes advanced energy management techniques and renewable energy sources, such as photovoltaic (PV) systems [8].

This paper focuses on integrating DC power generation systems into power plants and designing battery energy storage systems using multi-port converters [9,10]. It explores vehicle-to-home (V2H) scenarios, where plug-in electric vehicles (PEVs) act as backup power sources and home batteries during power outages or distribution failures, while also enabling efficient EV charging [10-12]. The paper aims to enhance performance using space vector modulation techniques and multiple converter analog (PCMM) to improve compensation. Additionally, the integration of artificial neural networks (ANN) is studied to enhance EV charging tracking, providing greater control and flexibility compared to traditional proportional-integral (PI) controllers [13,14].

To validate the feasibility and effectiveness of the system, both computational and experimental data are included. Results show that PCMM meets design objectives in home environments and operates effectively with a single electronic management system (EMS) [15]. This research supports the development of more powerful and sustainable EVs, promotes energy efficiency, and advances the transition toward a more energy-efficient future.

II. PROPOSED SYSTEM DESCRIPTION

This paper presents an advanced EV charging system using a SEPIC-Zeta converter optimized with the Wild Horse Algorithm for PI control is shown in figure 1. The system integrates a photovoltaic (PV) energy source with a bidirectional DC-DC converter, improving energy efficiency and voltage regulation over traditional converters. Pulse-width modulation (PWM) signals adjust the output voltage in real-time to ensure optimal charging. The Wild Horse Algorithm fine-tunes the PI controller to enhance transient

response and stability under varying voltages and loads. Additionally, a three-phase voltage source inverter (VSI) with an LC filter ensures clean, efficient energy delivery to the grid. This design improves energy management in EV charging stations and supports sustainable transportation infrastructure. The system is simulated and implemented using Matlab 2021a, proving its effectiveness in modern energy management.

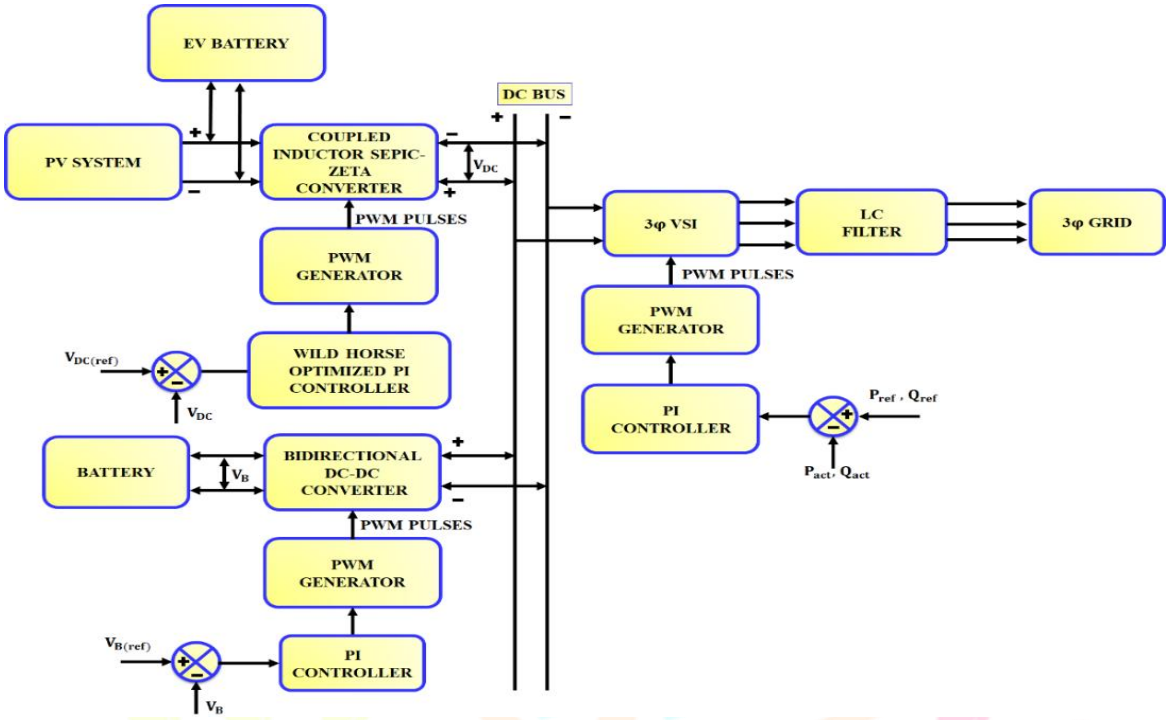

Figure 1. Block Diagram of Proposed System

A. PV System:

Solar panels in photovoltaic (PV) systems convert sunlight into electrical energy and its circuit is shown in figure 2. These panels are made up of photovoltaic cells, typically composed of silicon, which absorb sunlight. When sunlight strikes the cells, it excites electrons, causing them to flow and generate direct current (DC) electricity. This electron movement is the core process behind electricity generation in a PV system.

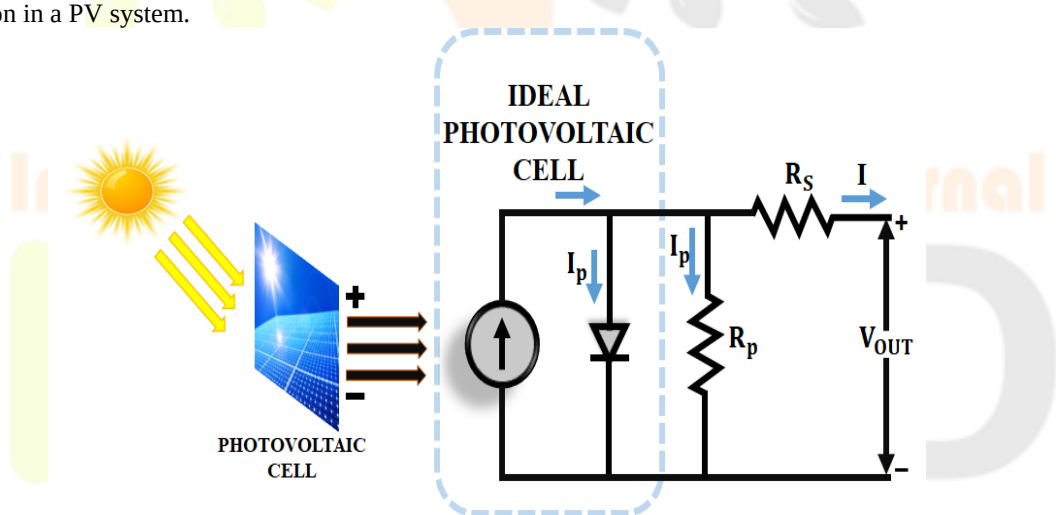

Figure 2. Circuit of PV System

The DC power generated by the solar panels is sent to an inverter, which converts it into alternating current (AC), the standard electricity used in homes and businesses. Inverters make the electricity compatible with the grid and household appliances. Once converted to AC, the energy can be used immediately by electrical devices, stored in batteries for later use, or fed back into the grid if there is excess. Advanced PV systems often include power controllers that monitor the flow of power to ensure efficiency and stability. Photovoltaic (PV) systems play a crucial role in renewable energy by converting sunlight into usable electricity, starting with solar panels capturing sunlight and generating DC power through the photovoltaic effect.

B. Coupled Inductor SEPIC Zeta Converter:

Coupled Inductors SEPIC (Single Ended Primary Inductor Converter) ZETA converters use two parallel magnetic inductors to effectively step up or step down while providing separate power applications. The circuit diagram of Coupled Inductor SEPIC Zeta Converter is shown in figure 3.

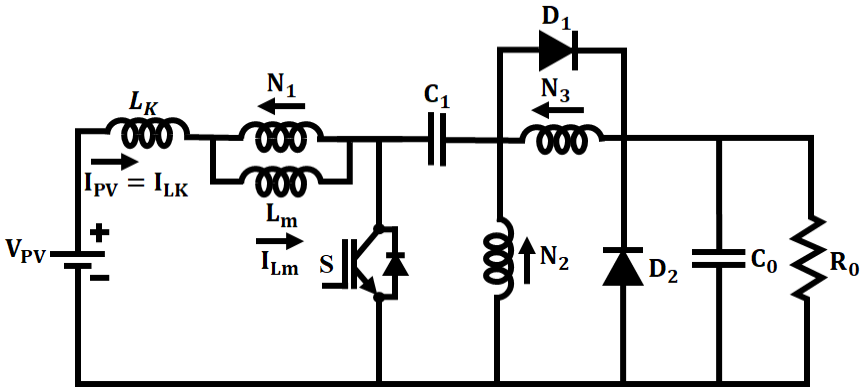

Figure 3. Coupled Inductor SEPIC Zeta Converter

In this converter, when a switch (usually a transistor) is activated, current flows through the primary winding of the coupled inductor, storing energy in its magnetic field. This causes a voltage in the secondary winding, increasing the output voltage. When the circuit is closed, the stored energy is released, causing current in the primary inductor to collapse and flow through the diode. This sends energy to the output capacitor and load, converting power. The coupled inductors help reduce voltage ripple and increase conversion efficiency, making SEPIC-ZETA converters ideal for DC-DC applications.

This converter is designed for efficient voltage regulation in renewable energy and battery charging systems, such as those used in electric vehicles (EVs) and solar PV systems. By combining ZETA and SEPIC converters, it allows the input voltage to be adjusted based on operating conditions, ensuring flexibility and stable output.

MODE 1:

In the initial mode, when switch S starts conducting, diode D_1 turns on while diode D_2 remains off. At this point, the input source charges the magnetizing inductance and releases the stored energy in capacitor. As switch S engages, current flows through the resistors, generating magnetic fields and transferring energy. This process allows the conversion of electrical energy into magnetic energy, which is stored in the inductance and later released to power the load.

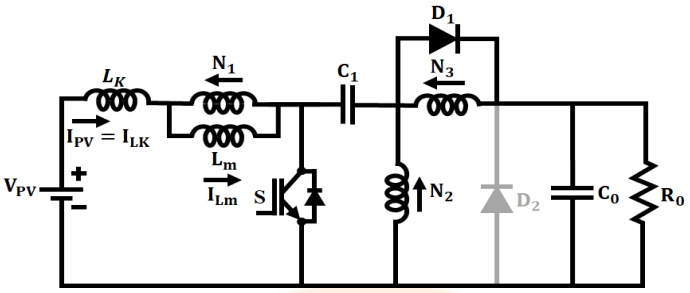

Figure 4. Mode 1 Operation

MODE 2:

In mode 2, diode D_1 and switch S are off, while diode D_2 is conducting. During this mode, capacitor C_1 is charged through the magnetizing inductor and diode D_1. Simultaneously, the output capacitor supplies power to the load. The mode concludes when the currents in both the leakage inductance and magnetizing inductance reach equilibrium, at which point energy transfer stabilizes, and the system is ready for the next switching cycle.

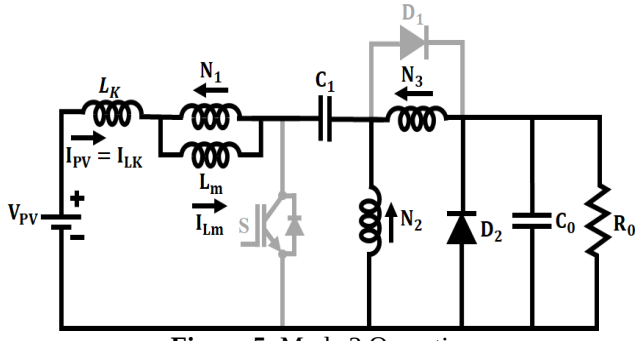

Figure 5. Mode 2 Operation

C. Bidirectional DC-DC Converter:

Bidirectional DC-DC converters enable energy conversion between two DC voltage sources for both charging and discharging, making them essential for applications such as electric vehicles and renewable energy systems. The use of diodes, inductors, or transformers provides the necessary bidirectional flexibility. The circuit diagram of Bidirectional DC-DC Converter is shown in figure 6.

In charge mode, the converter draws power from the DC bus or a regenerative power source and transfers it to the battery. Current flows through the inductor, storing energy in its magnetic field. When the circuit closes, energy flows to the battery. In discharge mode, power flows from the battery to the DC bus or load, with the converter adjusting the voltage as required.

The operation of the converter is controlled by a PI (proportional-integral) controller, which adjusts the duty cycle of the PWM (pulse width modulation) signals to ensure efficient energy transfer and maintain the desired voltage levels, optimizing the charging and discharging processes.

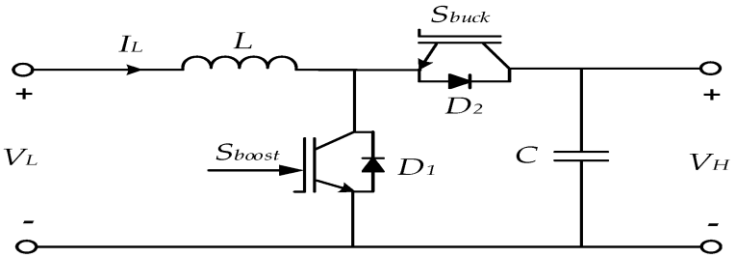

Figure 6. Bidirectional DC-DC Converter

Control Mechanism:

The bidirectional converter is controlled using pulse width modulation (PWM) signals, which regulate the switching of transistors (such as MOSFETs or IGBTs) to manage the direction and magnitude of the energy flow. A proportional-integral (PI) controller is typically employed to adjust the duty cycle of the PWM signals based on system feedback, ensuring that the voltage and current levels remain stable and within the desired range for efficient operation.

D. Wild Horse Optimized PI Controller:

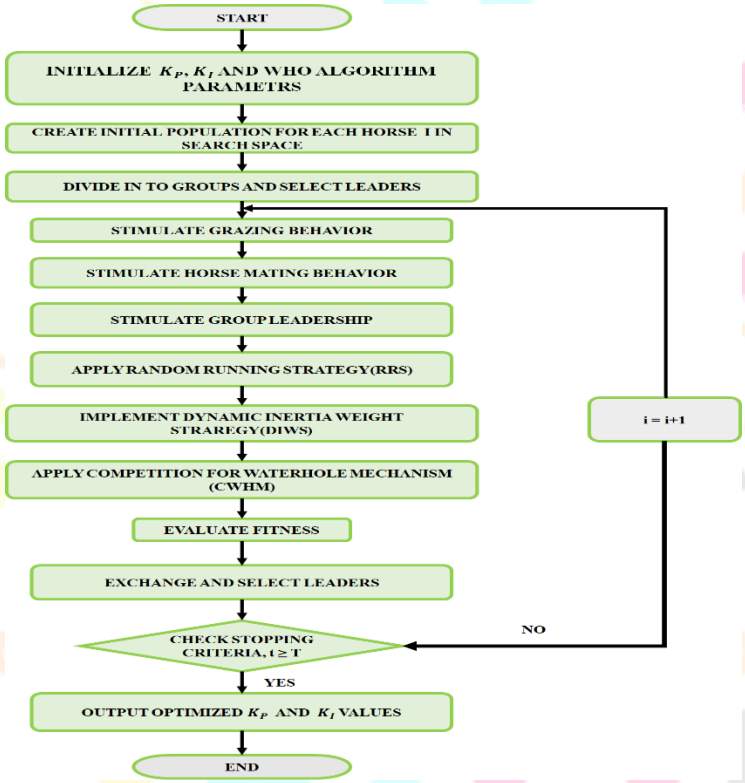

Figure 7. Wild Horse Optimized Flowchart

The Wild Horse Algorithm (WHA) optimizes the performance of the Proportional-Integral (PI) controller by tuning its parameters. WHA is a nature-inspired optimization technique that mimics the herding behavior of wild horses. In a PI controller, the proportional component addresses the current error, while the integral component corrects past accumulated errors. The effectiveness of the controller hinges on the precise adjustment of these parameters. The flow chart of this algorithm is shown in figure 7.

WHA works by initializing a population of potential solutions (horses) within a defined parameter space and evaluating their performance using a cost function, such as the Integral of Time-weighted Absolute Error (ITAE). The algorithm simulates the horses' natural exploration behavior, updating their positions iteratively to find better solutions until convergence is achieved.
This process enhances the PI controller's robustness, improves response times, and increases stability, making it well-suited for applications like renewable energy systems and industrial automation.

E. PI Controller

The proportional-integral (PI) controller is a popular feedback control system that regulates a process variable by combining integral and proportional actions. The circuit diagram of PI Controller is shown in figure 8.

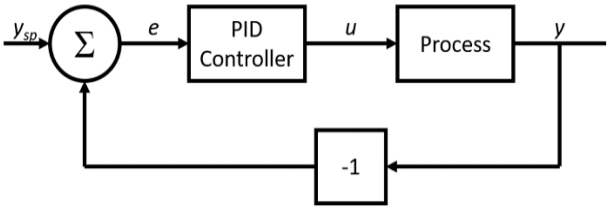

Figure 8. PI Controller

The integrated circuit responds immediately to changes by generating an output proportional to the current error. By adjusting the balance of proportional gain (Kp) and integral gain (Ki), the PI controller can be tuned for optimal stability and performance. This makes the PI controller highly effective for applications such as temperature control, speed regulation, and process automation. To achieve a balanced response and maintain stability, the controller's parameters, Kp and Ki, are carefully adjusted based on the system's requirements.

III. RESULTS AND DISCUSSIONS

The following outcomes are produced when the suggested task is implemented in Matlab Simulation. The Overall Simulation Block Diagram are shown in figure 9.

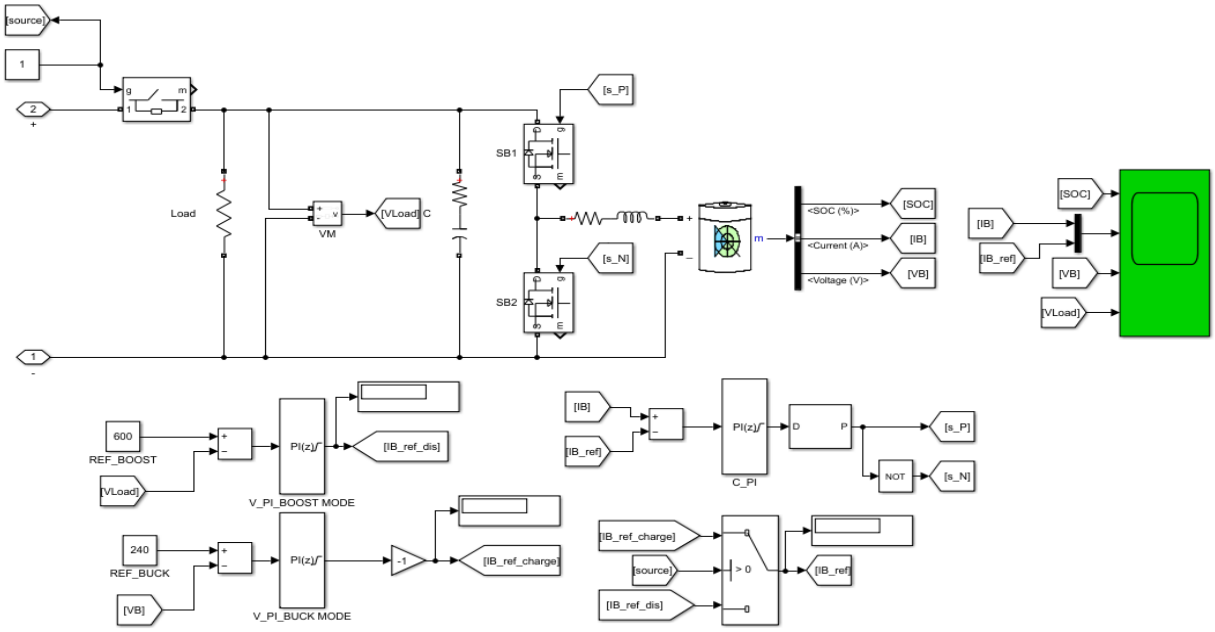

Figure 9. Overall Simulation Block Diagram

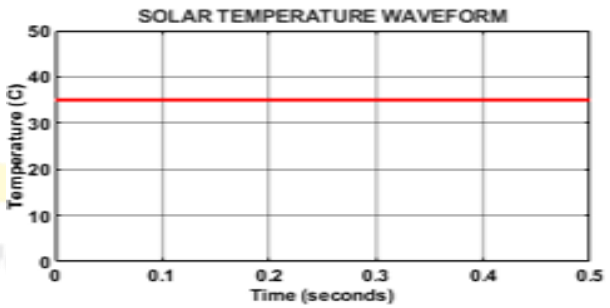

Figure 10. Solar Temperature Waveform

Figure 10 illustrates a constant temperature of approximately 35°C over a short time period from 0 to 0.5 seconds. The red line indicates that the temperature remains steady without fluctuation during this interval. The x-axis represents time in seconds, while the y-axis shows temperature in degrees Celsius.

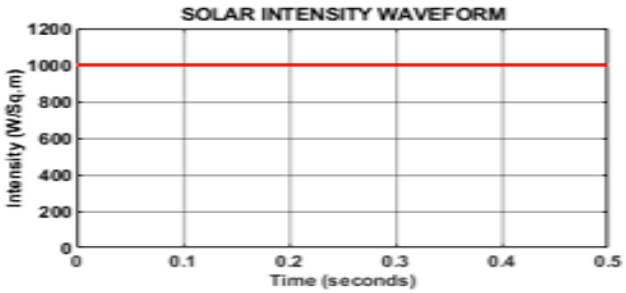

Figure 11. Solar Intensity Waveform

Figure 11 depicts the solar intensity waveform, showing a steady solar intensity of 1000 W/m² over a 0.5-second time span. The red line remains constant, indicating no variation in solar intensity throughout this interval. The x-axis represents time in seconds, and the y-axis shows intensity in watts per square meter.

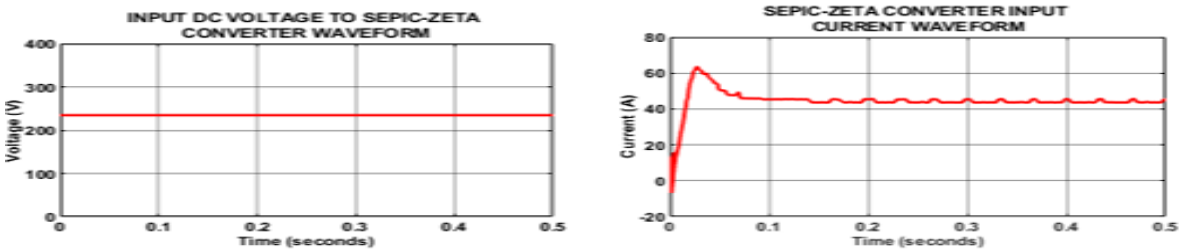

Figure 12. Input Waveform of Voltage & Current

Figure 12 shows the current and voltage waveforms of the SEPIC-Zeta Converter. The converter maintains a steady input DC voltage of approximately 200 volts over a 0.5-second period, ensuring stable operation. This consistent voltage is essential for the proper functioning of the converter.

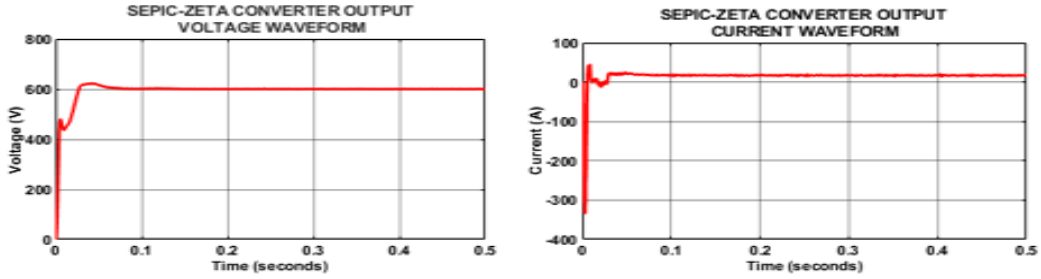

Figure 13. Output waveform of Voltage & Current

Figure 13 illustrates the output voltage and current waveforms of the SEPIC-Zeta Converter. The output voltage is steady at 800 mV, while the output current fluctuates between -300 mA and 100 mA before stabilizing. The voltage stabilizes quickly, while the current experiences slight fluctuations before reaching a steady state.

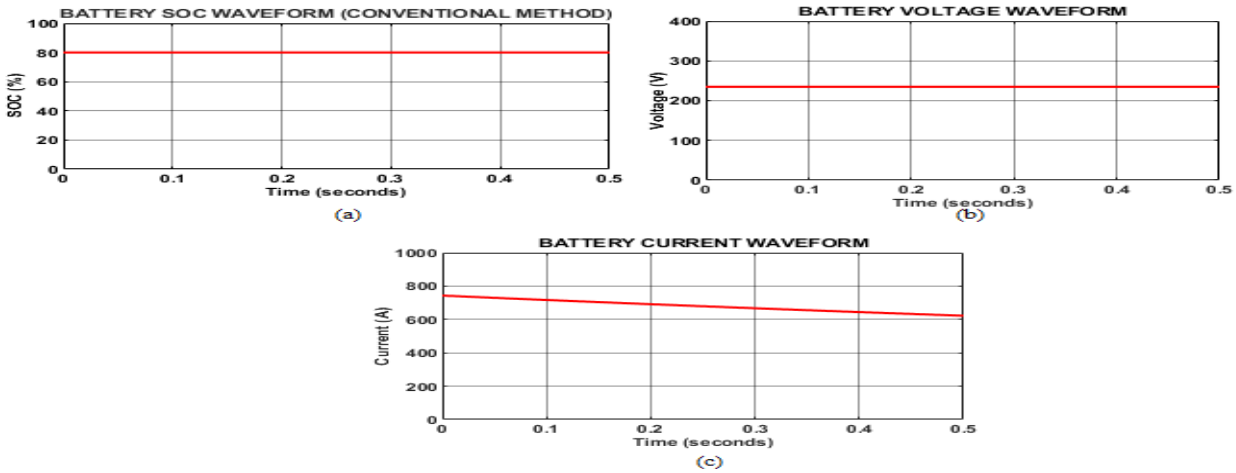

Figure 14. Battery's SOC, Voltage, and Current Waveform

Figure 14 presents the battery's state of charge (SOC), voltage, and current waveforms over time. The SOC remains constant at 100%, the voltage stays stable at 400V, and the current is steady at 0A, indicating no fluctuations during the observed period.

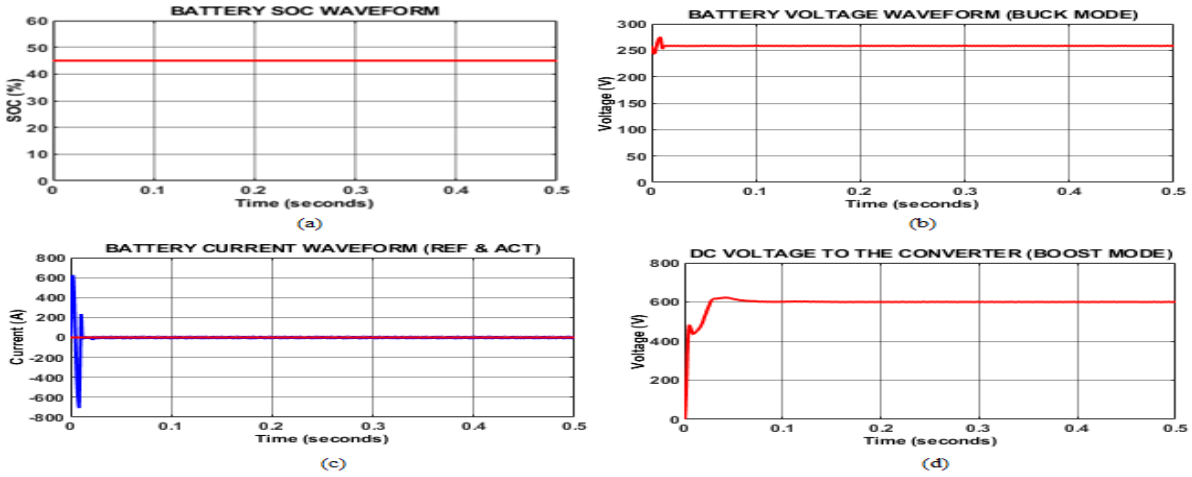

Figure 15. Waveform of Bidirectional Battery Converter

Figure 15 shows the bidirectional battery converter waveform. During the observed period, the battery's state of charge (SOC) remains at 80%, the voltage is steady at 200V in buck mode, the current stays at 100A, and the DC voltage to the converters is constant at 400V in boost mode. All parameters remain stable throughout the time.

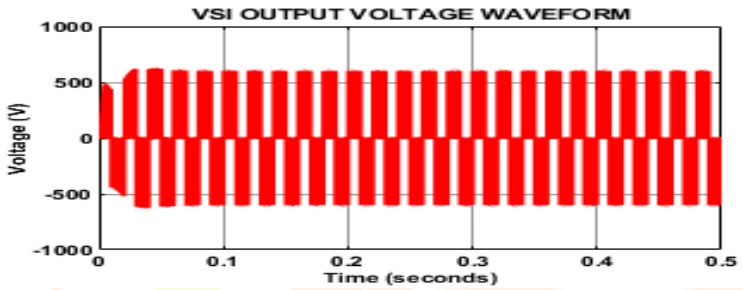

Figure 16. Waveform of VSI Output Voltage

Figure 16 illustrates the waveform of the VSI output voltage. The voltage alternates between +800V and -800V, forming a high-frequency square wave pattern. This behavior indicates efficient voltage regulation by the Voltage Source Inverter (VSI).

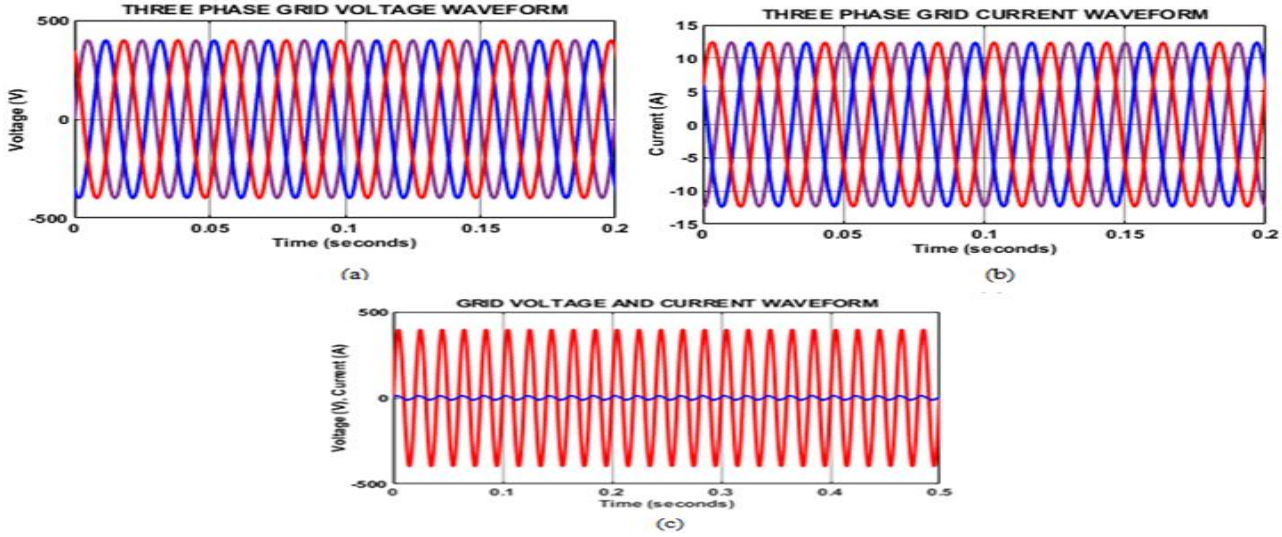

Figure 17. Waveform of Three Phase Grid

Figure 17 presents the waveform of the three-phase grid. The waveform monitors the voltage and current across the three-phase grid. The net voltage and current waveforms are analyzed to ensure the stability and efficiency of the system.

IV. CONCLUSION

In conclusion, this advanced EV charging solution utilizing a coupled inductor SEPIC-Zeta converter optimized by the Wild Horse Algorithm significantly enhances the efficiency and reliability of electric vehicle charging systems. By integrating a photovoltaic system with a bidirectional DC-DC converter, the architecture addresses energy conversion and voltage regulation challenges, improving EV battery charging performance. The dynamic adjustment of PWM signals ensures stable, efficient charging, while the Wild Horse Algorithm-optimized PI control offers robust response to varying conditions. Additionally, the three-phase VSI with an LC filter ensures high-quality energy delivery to the grid. This paper not only improves energy management in EV charging stations but also contributes to sustainable transportation, advancing the shift towards greener mobility. The successful implementation via Matlab Simulation 2021 highlights its real-world potential, making it a valuable innovation in renewable energy and electric mobility.

REFERENCES:

1. Sayed, M.A., Atallah, R., Assi, C. and Debbabi, M., 2022. Electric vehicle attack impact on power grid operation. International Journal of Electrical Power & Energy Systems, 137, p.107784.
2. Bin Ahmad, M.S., Pesyridis, A., Sphicas, P., Mahmoudzadeh Andwari, A., Gharehghani, A. and Vaglieco, B.M., 2022. Electric vehicle modelling for future technology and market penetration analysis. Frontiers in Mechanical Engineering, 8, p.896547.
3. Ravi, S.S. and Aziz, M., 2022. Utilization of electric vehicles for vehicle-to-grid services: Progress and perspectives. Energies, 15(2), p.589.
4. Wu, Y.C. and Kontou, E., 2022. Designing electric vehicle incentives to meet emission reduction targets. Transportation Research Part D: Transport and Environment, 107, p.103320.
5. Chen, J., Zhou, Z., Zhou, Z., Wang, X. and Liaw, B., 2022. Impact of battery cell imbalance on electric vehicle range. Green Energy and Intelligent Transportation, 1(3), p.100025.
6. E. Gümrükcü et al., "Optimal Management for Megawatt Level Electric Vehicle Charging Stations With a Grid Interface Based on Modular Multilevel Converter," in IEEE Access, vol. 10, pp. 258-270, 2022.
7. Hynynen, J., Willstrand, O., Blomqvist, P. and Andersson, P., 2023. Analysis of combustion gases from large-scale electric vehicle fire tests. Fire Safety Journal, 139, p.103829.
8. Szumska, E.M., 2023. Electric vehicle charging infrastructure along highways in the EU. Energies, 16(2), p.895.
9. Nazari, M., Hussain, A. and Musilek, P., 2023. Applications of clustering methods for different aspects of electric vehicles. Electronics, 12(4), p.790.
10. De Wolf, D. and Smeers, Y., 2023. Comparison of battery electric vehicles and fuel cell vehicles. World Electric Vehicle Journal, 14(9), p.262.
11. Liu, Y., Francis, A., Hollauer, C., Lawson, M.C., Shaikh, O., Cotsman, A., Bhardwaj, K., Banboukian, A., Li, M., Webb, A. and Asensio, O.I., 2023. Reliability of electric vehicle charging infrastructure: A cross-lingual deep learning approach. Communications in Transportation Research, 3, p.100095.
12. Alsharif, A., Tan, C.W., Ayop, R., Al Smin, A., Ali Ahmed, A., Kuwil, F.H. and Khaleel, M.M., 2023. Impact of electric Vehicle on residential power distribution considering energy management strategy and stochastic Monte Carlo algorithm. Energies, 16(3), p.1358.
13. C. Li et al., "Prediction of EV Charging Load Using Two-Stage Time Series Decomposition and DeepBiLSTM Model," in IEEE Access, vol. 11, pp. 72925-72941, 2023.
14. K. Vaishali and D. R. Prabha, "The Reliability and Economic Evaluation Approach for Various Configurations of EV Charging Stations," in IEEE Access, vol. 12, pp. 26267-26280, 2024.
15. Y. Gong and I. Kim, "Optimization and Observation of EV Charging Station Deployment in the Republic of Korea: An Analysis of the Charging History and Correlation With Socioeconomic Factors," in IEEE Access, vol. 12, pp. 68285-68302, 2024.